Materials Transactions, Vol. 43, No. 8 (2002) pp. 1864 to 1867
Special Issue on Lead-Free Electronics Packaging

Mechanical Properties and Shear Strength of Sn–3.5Ag–Bi Solder Alloys

Jin-Won Choi*, Ho-Seob Cha* and Tae-Sung Oh

Department of Metallurgical Engineering and Materials Science, Hong-Ik University, Seoul 121-791, Korea

Mechanical properties and ball shear strength of Sn–3.5Ag–Bi were investigated with Bi addition of 0–9 mass%. Solder characteristics of Sn–3.5Ag–Bi were improved with Bi addition to decrease the melting temperature, to promote wetting to Cu and Ni substrates, and to increase the tensile strength and fracture energy. Shear strength of Sn–3.5Ag–Bi solder bumps increased with Bi addition up to 5 mass%, and was kept almost unchanged with further increase of Bi addition. Shear strength exhibited a parabolic relationship with the tensile fracture energy of the solder alloys.

(Received February 18, 2002; Accepted June 18, 2002)

Keywords: *lead-free solder, tin-3.5silver-bismuth, tensile strength, solder bump, shear strength*

1. Introduction

Sn–Pb solders have been predominantly used as an interconnection and joining material in electronic packaging due to low melting temperatures, good mechanical properties, and excellent wettability. However, increased concerns for the environment have demanded the development of lead-free solders.[1–4] While investigations on lead-free solders were initiated by the legislative actions to ban Pb use, the electronic industry confronts lately much strong market pressure for development of lead-free solders from consumers desiring green electronic products.[3–5]

Among a number of lead-free solders have been developed,[1,2] Sn–3.5Ag eutectic solder is one of the attractive candidates to replace eutectic 63Sn–37Pb in many applications including low-cost electronic products like consumer electronics and computing devices.[1–4] Although the melting temperature of Sn–3.5Ag solder is relatively low compared to the melting points of other lead-free solders, it is still considerably higher than 183°C of 63Sn–37Pb eutectic solder.[1,2,6] Thus, many works have been conducted to modify the thermal and mechanical characteristics of Sn–3.5Ag solder with addition of Bi, Cu, Sb, In, and Zn as a ternary element.[1,3,5–8]

In this study, tensile strength and fracture energy of Sn–3.5Ag–Bi alloys were characterized with Bi addition up to 9 mass%. Sn–3.5Ag–Bi solder bumps were reflowed on BGA (Ball Grid Array) substrates with Au/Ni/Cu UBM (Under Bump Metallization), and their shear strengths were evaluated with the Bi content.

2. Experimental Procedure

Sn–3.5Ag–Bi alloys were prepared with Bi addition of 0–9 mass%. For all samples, the ratio of Ag to Sn was kept the same as the eutectic Sn–3.5Ag composition. Elemental metals were weighed for proper composition, charged in a quartz tube. The quartz tube was sealed under vacuum of 10^{-5} Pa, and the elemental metals were melt and homogeneously mixed at 800°C for 3 h using a rocking furnace. The ingot was remelted at 240°C for 30 min and cooled at the same rate of the reflow profile. The ingot was then machined to a tensile specimen (Fig. 1) and tensile test was carried out at a strain rate of 3×10^{-4}/s. Melting temperatures of Sn–3.5Ag–Bi solders were measured using DTA (Differential Temperature Analyzer).

To make the solder bumps, Sn–3.5Ag–Bi alloys were rolled to about 30 μm thickness and then manually punched out to make discs of 0.8 mm diameter. Sn–3.5Ag–Bi solder discs were reflowed at 240°C for 30 or 60 sec on Au (0.5 μm)/Ni (5 μm)/Cu (27 μm) UBM in a RMA flux ambient. Conventional BGA substrate, *i.e.*, photo solder resist (PSR)-defined UBM on bismaleimide triazine (BT)-resin substrate, was used in this study. Figure 2 shows a schematic illustration of a solder bump reflowed on BGA substrate with Au/Ni/Cu UBM.

Ball shear test was conducted using a Dage-2400 shear tester at a constant shear speed of 0.2 mm/s with a fixed shear tip height of 0.05 mm above the solder mask surface. For each experimental condition, more than 30 solder bumps were sheared off in accordance with the JEDEC standard.[9] Shear strength was obtained by dividing the shear force with

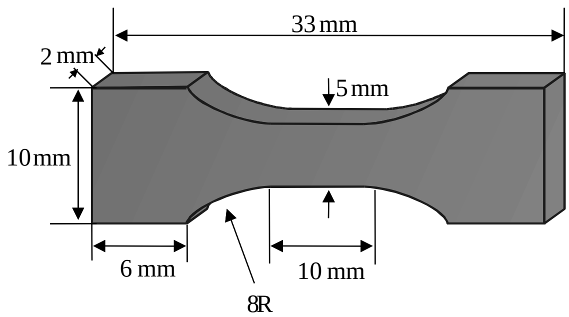

Fig. 1 Schematic illustration of a tensile specimen.

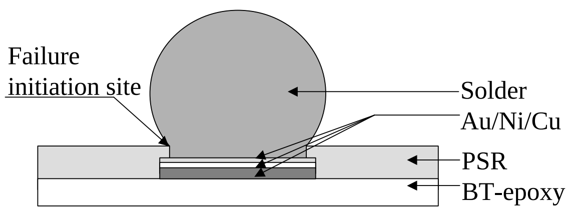

Fig. 2 Schematic illustration of a solder bump reflowed on Au/Ni/Cu UBM.

*Graduate student, Hong-Ik University.

the UBM pad area. Microstructure of Sn–3.5Ag–Bi alloys and solder bumps were observed using Scanning electron microscopy (SEM) with Backscattered electron image (BEI).

3. Results and Discussion

3.1 Characteristics of Sn–3.5Ag–Bi solder alloys

Figure 3 shows the melting point of Sn–3.5Ag–Bi solder alloys. The melting point of Sn–3.5Ag–Bi decreased linearly with increasing the Bi content, from 221°C of Sn–3.5Ag to 210°C of Sn–3.5Ag–9Bi. Sn–3.5Ag–Bi alloy with Bi content more than 3 mass% exhibited a melting point lower than 217°C of the ternary eutectic Sn–Ag–Cu alloy.[1] Figure 4 illustrates the wetting angle of Sn–3.5Ag–Bi solder on Cu and Ni substrates. The wetting angles on Ni substrate as well as on Cu substrate decreased continuously with increasing the Bi addition, which could be attributed to a decrease in the solder-flux interfacial tension with increasing the amount of Bi addition.[6]

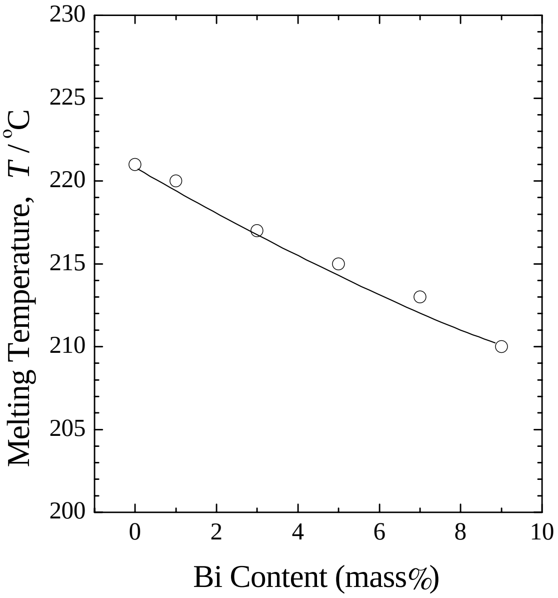

Fig. 3 Melting point of Sn–3.5Ag–Bi alloys as a function of the Bi content.

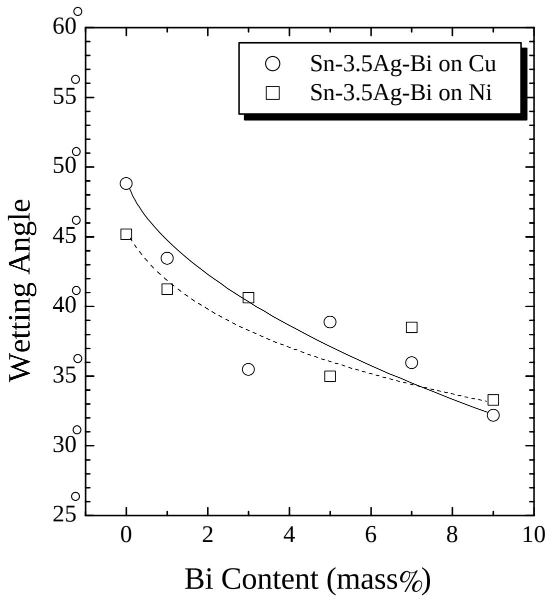

Fig. 4 Wetting angle of Sn–3.5Ag–Bi alloys on Cu and Ni substrates.

Figure 5 shows the tensile strength of Sn–3.5Ag–Bi solder alloys as a function of the Bi content. Tensile strength increased with increasing the Bi content. While the increase in the tensile strength with Bi addition less than 5 mass%, the solubility limit of Bi in Sn, could be due to solid solution hardening, further strength increment with Bi addition beyond its solubility limit would be attributed to Bi precipitation.[7,8] Figure 6 shows SEM micrographs of Sn–3.5Ag–Bi solder alloys. Bi precipitates were clearly observed for Sn–3.5Ag–Bi alloys with Bi content more than 3 mass%. Xiao *et al.*[10] also observed an increase in tensile strength of Sn–Ag alloy with Bi addition and reported with TEM analysis that the strength increase in Sn–3.4Ag–4.8Bi alloy was caused by Bi precipitation.

Figure 7 shows the fracture energy of Sn–3.5Ag–Bi solder alloys as a function of the Bi content. The fracture energy was calculated from the integral of the area under the stress-strain curve. The fracture energy of Sn–3.5Ag–Bi alloys also increased with increasing the Bi addition. However, the increment of the fracture energy was less than that of the tensile strength due to the decrease in ductility with increasing the Bi content. It has been suggested that the decrease in the ductility of Sn–3.5Ag–Bi alloys is caused by the irregularly shaped Ag_3Sn second phase particles in the Sn-rich matrix.[8]

Our results on Sn–3.5Ag–Bi solder alloys confirmed that the solder characteristics of Sn–3.5Ag can be improved with Bi addition to decrease the melting temperature, to promote wetting to Cu and Ni substrates, and to increase the strength and fracture energy.

3.2 Shear strength and fracture behavior of Sn–3.5Ag–Bi solder bumps

Figure 8 shows the shear strength of Sn–3.5Ag–Bi solder bumps with variation of the Bi content. To prepare the solder bumps, Sn–3.5Ag–Bi solder discs of 0.8 mm diameter were reflowed on 0.64 mm Au/Ni/Cu UBM for 30 and 60 s. The

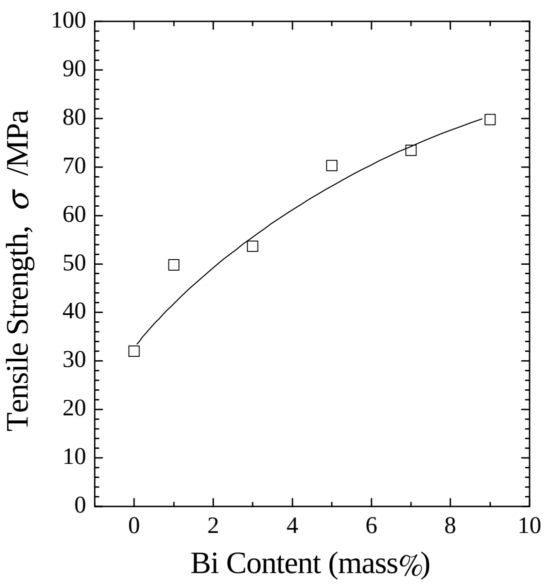

Fig. 5 Tensile strength of Sn–3.5Ag–Bi alloys as a function of the Bi content.

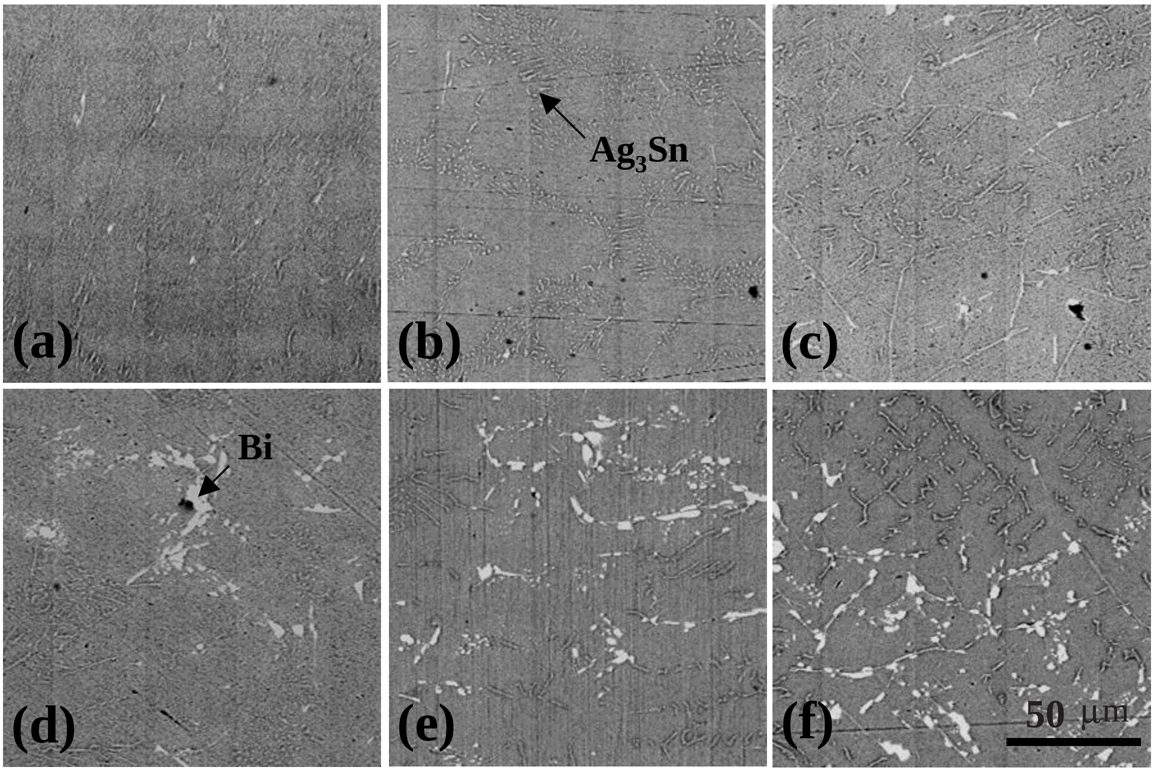

Fig. 6 SEM micrographs of Sn–3.5Ag–Bi alloys with Bi content of (a) 0 mass%, (b) 1 mass%, (c) 3 mass%, (d) 5 mass%, (e) 7 mass%, and (f) 9 mass%.

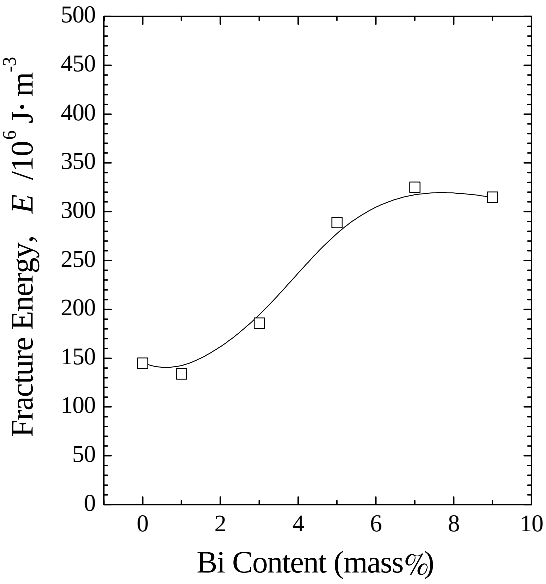

Fig. 7 Fracture energy of Sn–3.5Ag–Bi alloys as a function of the Bi content.

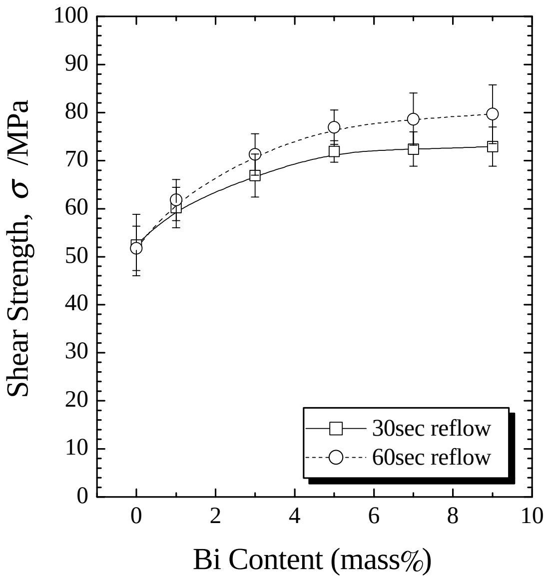

Fig. 8 Shear strength of Sn–3.5Ag–Bi solder bumps, reflowed on Au/Ni/Cu for 30 and 60 seconds, as a function of the Bi content.

shear strength of the solder bumps increased with Bi addition up to 5 mass%, and was kept almost unchanged with further increase of Bi addition.

During ball shear test, ductile fracture occurred in the solder for all the solder bumps with 0–9 mass% Bi addition regardless of the reflow time of 30 or 60 s. As the shear crack propagated in the solder, the shear strength of the solder bumps should be related to the mechanical properties of the solder alloys. As shown in Fig. 5, tensile strength of Sn–3.5Ag–Bi alloys increased by solid solution hardening with Bi addition less than 5 mass%, and by dispersion hardening of Bi precipitates with Bi addition beyond its solubility limit.[7,8] With applying such strengthening mechanisms to the shear strength change of the solder bumps (Fig. 8), it seems that dispersion hardening with Bi precipitates is not as effective as solid solution hardening is to improve the shear strength of Sn–3.5Ag–Bi solder bumps. Considering adverse effect of Bi addition on thermal fatigue,[8,11] Bi addition in Sn–3.5Ag–Bi can be suggested to be less than 5 mass% for the solder bumping process.

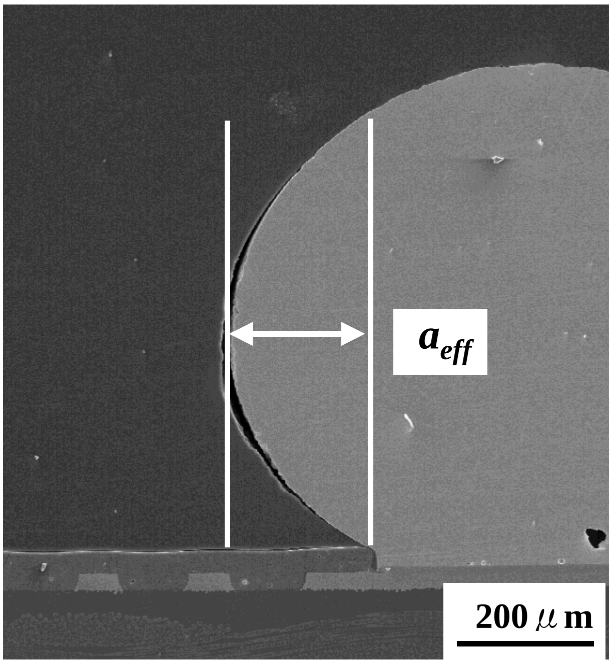

Fig. 9 Cross-sectional SEM micrograph of the Sn–3.5Ag–Bi solder bump.

During ball shear test, shear mode loading is applied to the solder bump and the neck edge corner shown in Fig. 1 acts as a notch crack tip where the solder joint failure initiates. As shown in Fig. 9, the distance from the contact point of the bump-shear tip to the neck edge corner may be defined as the effective crack size a_{eff} for shear-mode fracture. As the solder is soft at room temperature, however, plastic deformation at the neck edge corner occurs freely and the plastic zone spreads through the entire area of the solder bump adjacent to the bump/UBM interface. With large scale plasticity during ball shear test, thus, linear elastic fracture mechanics with the effective crack size a_{eff} are not applicable, but J integral should be used for the shear-mode fracture of the solder bump.

As shown in Fig. 8, the shear strength was improved by increasing the reflow time from 30 to 60 s for all compositions of the solder bumps. Such increase in the shear strength could be related to dissolution of Ni in Au/Ni/Cu UBM to the solder during reflow. As reported for 63Sn–37Pb reflow,[12] Au layer in Au/Ni/Cu UBM is dissolved completely into Sn–3.5Ag during reflow, exposing Ni layer to the molten solder.[13,14] Contrary to low solubility limit of Ni, 0.052 at%, in 63Sn–37Pb at 220°C, solubility limit of Ni in Sn–3.5Ag at 250°C is relatively high (0.28 at%).[15] However, the dissolution rate of Ni into Sn-rich solders is slow,[15] and the amount of Ni dissolved into Sn–3.5Ag–Bi would increase with increasing the reflow time from 30 to 60 s in this study. This might cause the solid solution hardening effect of Ni and increase the shear strength of the Sn–3.5Ag–Bi after reflowing for 60 s.

4. Conclusions

With studying on the mechanical properties of Sn–3.5Ag–Bi alloys and the shear strength of Sn–3.5Ag–Bi solder bumps reflowed on Au/Ni/Cu UBM, the following conclusions could be made:

(1) Melting point of Sn–3.5Ag–Bi decreased linearly with increasing the Bi content, from 221°C of Sn–3.5Ag to 210°C of Sn–3.5Ag–9Bi. Wetting angle of Sn–3.5Ag–Bi decreased continuously on Cu and Ni substrates with increasing the Bi addition.

(2) Tensile strength and fracture energy of Sn–3.5Ag–Bi alloys increased with increasing the Bi addition. However, the increment of the fracture energy was less than that of the tensile strength due to the decrease in ductility with Bi addition.

(3) Shear strength of Sn–3.5Ag–Bi solder bumps increased with Bi addition up to 5 mass%, and was kept almost unchanged with further increase of Bi addition. Dispersion hardening with Bi precipitates may not be as effective as solid solution hardening to improve the shear strength of solder bumps, and Bi addition in Sn–3.5Ag–Bi can be suggested to be less than 5 mass%.

Acknowledgements

This work was supported by Center for Electronic Packaging Materials of Korea Science and Engineering Foundation.

REFERENCES

1) K. Suganuma: Solid State Mater. Sci. **5** (2001) 55–64.
2) M. Abtew and G. Selvaduray: Mater. Sci. Eng. **27** (2000) 95–141.
3) J. W. Jang, D. R. Frear, T. Y. Lee and K. N. Tu: J. Appl. Phys. **88** (2000) 6359–6363.
4) S. K. Kang, D. Y. Shih, K. Fogel, P. Lauro, M. J. Yim, G. Advocate, M. Griffin, C. Goldsmith, D. W. Henderson, T. Gosselin, D. King, J. Konrad, A. Sarkhel and K. J. Putlitz: *Proc. 51st Electronic Components and Technol. Conf.*, (IEEE, 2001) pp. 448–454.
5) E. Bradley III and J. Hranisavljevic: *Proc. 50th Electronic Components and Technol. Conf.*, (IEEE, 2000) pp. 1443–1448.
6) P. T. Vianco and J. A. Rejent: J. Electron. Mater. **28** (1999) 1127–1132.
7) P. T. Vianco and J. A. Rejent: J. Electron. Mater. **28** (1999) 1138–1143.
8) Y. Kariya and M. Otsuka: J. Electron. Mater. **27** (1997) 866–870.
9) JESD22-B117 "BGA Ball Shear," July 2000, JEDEC Solid State Technology Association.
10) L. Xiao, J. Liu, Z. Lai, L. Ye and A. Tholen: *Proc. Int. Symp. Adv. Packaging Mater.*, (International Microelectronics & Packaging Society, 2000) pp. 145–151.
11) J. R. Oliver, J. Liu and Z. Lai: *Proc. Int. Symp. Adv. Packaging Mater.*, (International Microelectronics & Packaging Society, 2000) pp. 152–156.
12) A. Zribi, R. R. Chromik, R. Presthus, J. Clum, K. Teed, L. Zavalij, J. De Vita, J. Tova and E. J. Cotts: *Proc. IEEE/CPMT Int. Electronics Manufacturing Technol. Symp.*, (IEEE, 1999) pp. 451–457.
13) K. Y. Lee and M. Li: Metall. Mater. Trans. **32A** (2001) 2666–2668.
14) K. Y. Lee, M. Li, D. R. Olsen, W. T. Chen, B. T. C. Tan and S. Mhaisalkar: *Proc. 51st Electronic Components Technol. Conf.*, (IEEE, 2001) pp. 478–485.
15) K. Zeng and K. N. Tu: "*Reliability Issues of Pb-free Solder Joints in Electronic Packaging Technology*," submitted to Mater. Sci. Eng. (2001).